An unsaturated soil mechanics approach for performance-based intelligent compaction

Liuxin Chen[1*], *Javad* Ghorbani[1], *Amir* Tophel[1], and *Jayantha* Kodikara[1]

[1]ARC Industrial Transformation Research Hub (ITRH) – SPARC Hub, Dept. of Civil Engineering, Monash University, Clayton Campus, VIC 3800, Australia

Abstract. Intelligent compaction involves using instrumented rollers to provide real-time monitoring of the compacted ground using sensors such as accelerometers and GPS. This technology has the potential to improve productivity and uniformity in construction but its advancement is currently impeded due to inaccurate estimation of the physical ground properties, such as dry density, and the absence of robust quantitative models to predict the effect of compaction on the long-term performance of unsaturated soils under repeated loads. In this study, the compaction of the soil layers and subsequent deformations under repeated traffic loads are simulated by using an advanced computational framework and model for unsaturated soils. By employing an effective stress concept, the presented computational approach allows a unified description of soils at various degrees of saturation. In addition, the model can capture plastic deformations at the initiation of loading and thereby offer accurate predictions of soil behaviour under cyclic loads. Several numerical examples will be provided to demonstrate how the initial states of compacted soils affect the compaction efficiency and the long-term performance of compacted soils.

1 Introduction

Intelligent Compaction (IC), which is performed by an instrumented vibratory drum, offers a real-time and complete evaluation of compaction quality. More recently, the technology also allows automatic adjustments to the compaction process [1]. This technology aims to optimise compaction by potentially avoiding over-compaction and under-compaction, providing uniform compacted layers, and minimising the number of roller passes. Despite these signs of progress, the technology is under criticism for a lack of robust connection between the actual soil properties, such as dry density (or void ratio), and the measurements.

Since the void ratio is a fundamental state parameter of the soil, to establish scientifically sound approaches to the performance of compacted soils, IC can be further advanced by predicting ahead of time changes in density or void ratio Δe during compaction as well as during operation. In addition, as highlighted by the researchers [2,3], the degree of saturation S_r, which is determined by $S_r = G_s w/e$ (where G_s, w and e are specific gravity, moisture content and void ratio, respectively), is important for compaction quality control. Hence gaining insights into how S_r influences the deformations of compacted layers should also benefit the IC technology as the operator can adjust parameters such as the roller speed and the vibration amplitude of the drum to avoid over-compaction and under-compaction. This paper proposes a numerical approach that employs an unsaturated soil constitutive model to simulate the compaction of soil layers and subsequent deformations under traffic loads after construction with a particular emphasis on the role of soil initial states (e.g., initial void ratio e_0 and initial degree of saturation S_{r0}) in these processes. Several numerical examples are carried out to demonstrate the influence of soil initial states on the performance of road pavements.

2 Unsaturated soil mechanics approach

We use the model proposed by Chen et al. [4], which is based on the effective stress concept and multi-surface plasticity, to obtain soil constitutive relations. The model is selected because of the following model features which considerably facilitate the numerical modelling for the IC process and the long-term performance of the compacted soils under repeated traffic loads:

1) Unified description of unsaturated soil behaviour for various soil types and degrees of saturation. This feature is advantageous since the soils in the field are usually multi-layered systems with various degrees of saturation and various soil types under diverse loading conditions (including cyclic loads). The feature is partially attributed to the employed effective stress concept, which allows smooth transitions to Terzaghi's effective stress when the degree of saturation increases to unity and the generalization of many well-established theories in saturated soils (e.g., the critical state theory) to

* Corresponding author: Liuxin.Chen@monash.edu

partially saturated states [5]. In addition, the volumetric hardening law employs the concept of the Limiting Compression Curve (LCC), which guarantees that predicted isotropic compression lines reach the LCC at a high-stress level, as corroborated by the test results [6]. The LCC concept enables the unified description of different types of soils, such as sand, clay and silt.

2) Enhanced prediction of ratcheting of soils subjected to cyclic loads. It should be noted that many models use a yield surface and decompose the stress-strain path into a purely elastic region and an elastoplastic region beyond the yield surface [7]. These models often predict no plastic deformations when the stress state is within the yield surface. The prediction is inconsistent with the experimental results [8] and can be an obstacle to the accurate prediction of ratcheting of soils under cyclic loads. To have an enhanced prediction of cyclic behaviour, the model [4] employs the multi-surface concept with the postulation of no demarcation for purely-elastic and elastoplastic regions. In addition, the volumetric hardening law in the model is formulated in a way that guarantees a smooth change from a nearly elastic response at low-stress levels to the LCC at high-stress levels where the crushing of particles may occur.
3) Incorporation of the effect of stress-induced anisotropy on the volumetric hardening law. This feature is important since it can generalise the volumetric hardening law to the cases where soil undergoes anisotropic compression, e.g., one-dimensional (1-D) compression.
4) The capability of capturing initial experimentally-observed reduction in the degree of saturation upon constant suction compression and offering reasonable predictions of the soil response at a high-suction level. The Soil Water Retention Curve (SWRC) is formulated by considering both hysteresis feature of SWRCs and the effect of volume changes on SWRCs. The SWCC formulations can be found in Chen et al. [4] and will not be repeated here.

A brief description of the model is given as follows. The elastic bulk modulus K is given by:

$$K = K_0 p_a \frac{1+e}{e}\left(\frac{p'}{p_a}\right)^c \quad (1)$$

where p_a is atmospheric pressure. In addition, c and K_0 are fitting parameters.

By utilising the concept of LCC for saturated soils [9], the mean effective stress and the normalisation approach proposed by Tarantino and De Col [10], the generalised LCC for saturated and unsaturated soils under isotropic compression is formulated by:

$$\ln e = \ln(e_0^{sat}) - \lambda \ln(p') + \ln\left(1 + a\left(\frac{s^*}{p'}\right)^b\right) \quad (2)$$

where p' is mean effective stress; and s^* is the modified suction defined by $s^* = sn$ (where s is suction and n is porosity). In addition, e_0^{sat}, λ, a and b are model parameters.

Following Pestana and Whittle [11] and Ghorbani and Airey [12], the volume change is formulated by interpolating the elastic volume change ($\mathrm{d}\varepsilon_v^e$) and the volume change on the LCC ($\mathrm{d}\varepsilon_v^{LCC}$), as shown in Eq. (3).

$$\mathrm{d}\varepsilon_v = I(\delta_p)\mathrm{d}\varepsilon_v^{LCC} + \left(1 - I(\delta_p)\right)\mathrm{d}\varepsilon_v^e \quad (3)$$

where $I(\delta_p)$ is an interpolation function given by the researchers [4]:

$$I(\delta_p) = 1 - \mathrm{sign}(\delta_p)\,|\delta_p|^\theta;\ \ 0 < \theta < 1 \quad (4)$$

where θ is a model parameter; $\mathrm{sign}(*)$ is the sign function; and δ_p is a reference index that indicates the distance from the current mean effective stress to the image point on the LCC. Under isotropic compression, the image point is denoted by $\bar{p}'$ and δ_p is defined by:

$$\delta_p = 1 - \frac{p'}{\bar{p}'} \quad (5)$$

and in the case of anisotropic compression, the image point is denoted by $\bar{p}'_{an}$ and δ_p is defined by Pestana and Whittle [9] as:

$$\delta_p = 1 - \frac{p'}{\bar{p}'_{an}} \quad (6)$$

where the relationship between $\bar{p}'_{an}$ and $\bar{p}'$ is shown in Eq. (7) to quantify the effects of stress-induced anisotropy based on experimental observations.

$$\bar{p}'_{an} = \frac{\bar{p}'}{\left(1 + 2\frac{\eta^2}{M^2}\right)} \quad (7)$$

where η is the stress ratio obtained from $\eta = q/p'$ with q representing deviatoric stress. In addition, M denotes the slope of the critical state line in the $(q - p')$ plane. The schematic representation of the soil volume changes under anisotropic compression is illustrated in Fig. 1. It should be highlighted that the reference index δ_p is approximately one when the current stress state is far away from the LCC and the soil exhibits nearly elastic behaviour. As δ_p decreases, the stress state is getting closer to the LCC. When δ_p is reduced to zero, the stress state reaches the LCC. In this scenario, the compression curve follows the LCC, signifying the soil experiences a high-stress level where fragmentation of particles is likely to happen.

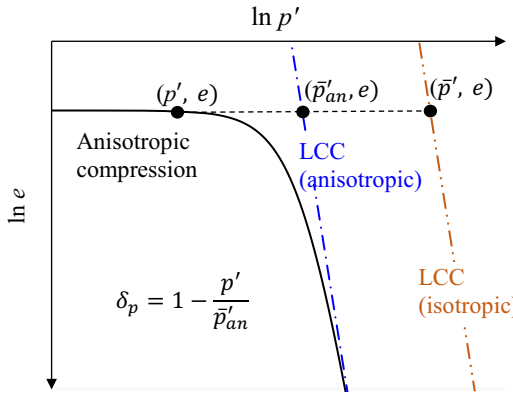

Fig. 1. Anisotropic compression and associated model components

3 Simulation of compaction and traffic loads

The numerical simulations of the compaction process were conducted with several assumptions that were made by Tophel et al. [13] to simplify the modelling process yet maintain the essential features of IC. The assumptions are as follows.

1) The interaction between a cylindrical drum (which can be assumed rigid relative to the soil) and the soil is an example of contact between nonconforming grids where contact pressure depends on a number of factors, such as initial void ratio and degree of saturation [14]. Nonetheless, in the presented work, as a key simplifying assumption, it is assumed that a maximum and fixed stress amplitude of around 1 MPa is transferred to the soil domain during compaction.
2) The frequency of rollers is typically between 18–30 Hz, which generates the application of vertical net stress with an amplitude of vibratory stress σ_V around an average of static stress σ_S, as shown in Fig. 2.
3) We considered a condition of constant water content during compaction given the fact that perfect drainage is usually not possible during vibration [14].
4) The compaction and post-compaction processes are approximated under 1-D conditions.

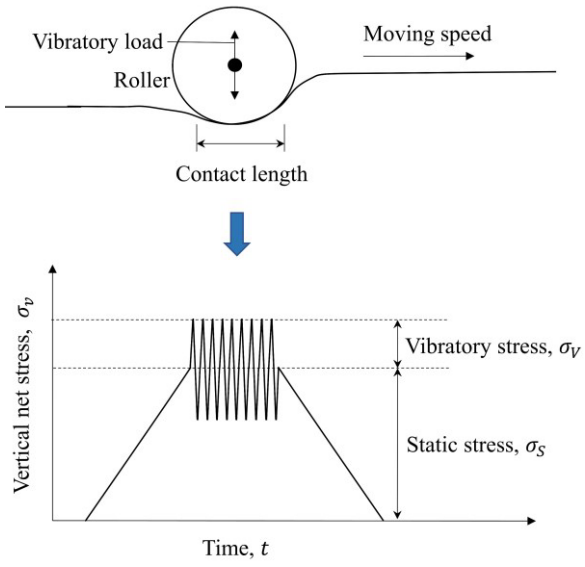

Fig. 2. Sketch of the compaction process and the simplified loading conditions during compaction

Based on the aforesaid assumptions and the model proposed by Chen et al. [4], various sets of numerical analyses with different e_0 and S_{r0} were conducted. For calibration and validation purposes, we selected the constant water content 1-D laboratory tests [13] which simulate the field compaction. The soil tested is a uniformly graded fine sand with G_s=2.61. In each set of analyses, we simulated the compaction process involving 10 roller passes at a constant w. Each roller pass contains 9 cycles with σ_V=280 kPa and σ_S=840 kPa. The model parameters were calibrated based on the procedure outlined by Chen et al. [4] with the same notations. Since no tests are conducted for the soil water retention behaviour, the SWRC parameters are back-calculated based on the available test results. The used model parameters are listed in Table 1.

Table 1. Used model parameters

Parameter		value
Elasticity	K_0	237
	c	0.67
Volumetric hardening	e_0^{sat}	0.689
	λ	0.018
	θ	0.04
Unsaturated state	a	0.21
	b	0.18
Critical state	M	1.278
SWRC	M_s	-1.8*
	$\lambda_d = \lambda_w$	0.28*
	λ_h	0.008*
	λ_{h1}	0*
	D_H/kPa	-189*
	$\beta_d = \beta_{w1}$	5*
	β_w	12*
	S_r^{sat}	0.93*

Note that the superscript (*) denotes an assumed value due to insufficient data.

In the simulations, the initial hydraulic state is postulated to be on the main drying curve. The evolution of suction is obtained from the SWRCs based on e and S_r. As an example, soil hydraulic states at the beginning and the end of the analysis where e_0=0.772, w=0.1 and S_{r0}=0.34 are illustrated in Fig. 3. As can be seen in the graph, at the end of the analysis, the hydraulic state passes through the scanning curve. In addition, the evolution of suction in the same analysis is shown in Fig. 4, which reflects the hysteresis of SWRC and the dependence of SWRC on the volume changes. The typical predicted void ratio during compaction is compared with the laboratory test data documented by Tophel et al. [13], as presented in Fig. 5 and Fig. 6. Good agreement between the predicted and test results can be seen in these two figures, demonstrating the effectiveness of the model in simulating compaction.

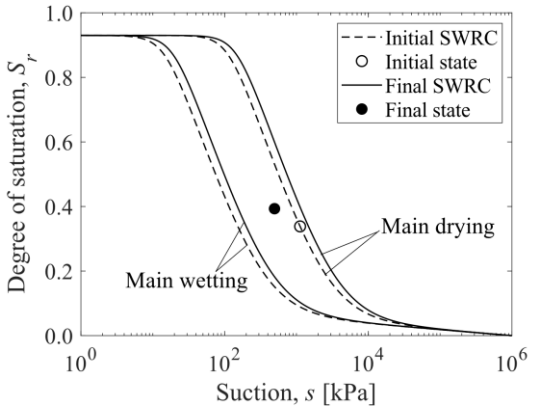

Fig. 3. Hydraulic states at the start and the end of the analysis (where e_0=0.772, w=0.1 and S_{r0}=0.34)

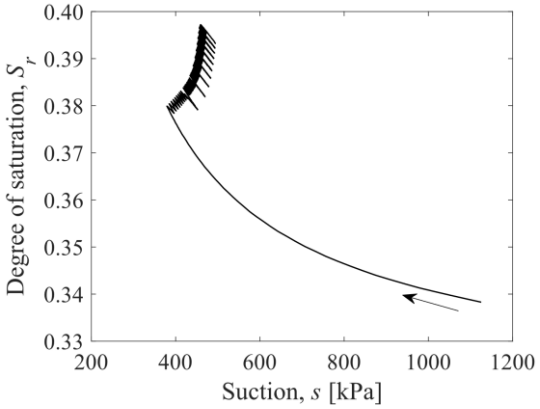

Fig. 4. Suction evolution in the analysis where e_0=0.772, w=0.1 and S_{r0}=0.34

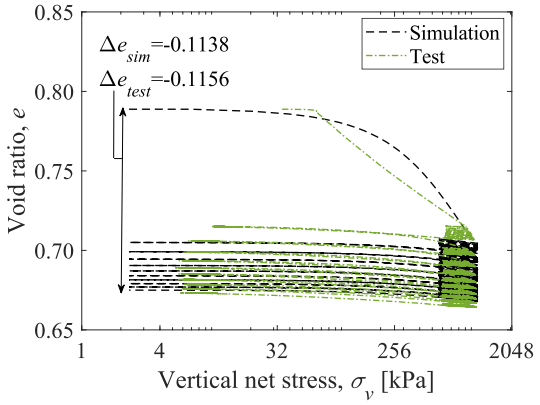

Fig. 5. Simulation for compaction against the laboratory test results from Tophel et al. [13] (where e_0=0.789, w=0.05 and S_{r0}=0.17)

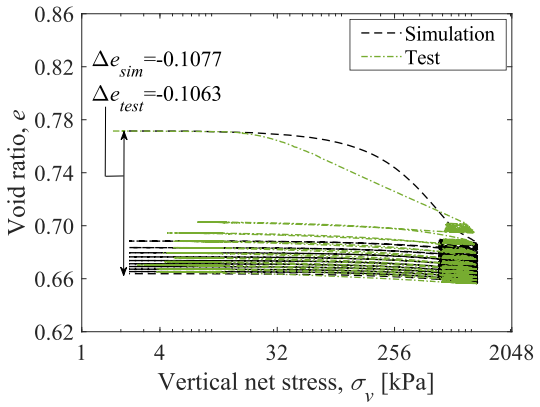

Fig. 6. Simulation for compaction against the laboratory test results from Tophel et al. [13] (where e_0=0.772, w=0.1 and S_{r0}=0.34)

The traffic loads are simulated by considering 100 cycles of repeated loads with a maximum σ_v of 400 kPa and a minimum σ_v of 2 kPa. A numerical example showing soil void ratio changes under traffic loads after compaction is provided in Fig. 7.

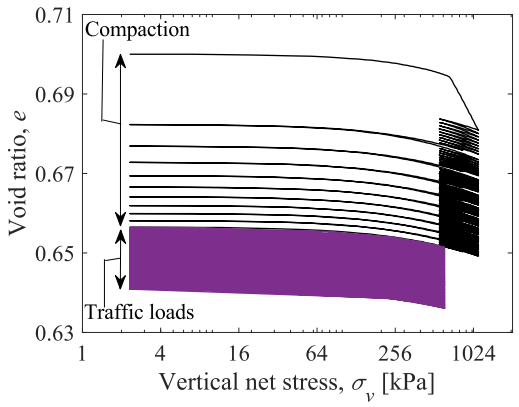

Fig. 7. Model predictions for compaction and traffic loads (where e_0=0.7, w=0.16 and S_{r0}=0.6)

4 Effects of the initial states of compacted soils

By using the unsaturated soil mechanics approach in Section 2 and the assumptions listed in Section 3, 18 numerical examples were performed to investigate how the initial states of compacted soils affect the compaction efficiency (see Section 4.1) and the long-term performance of the compacted soils under traffic loads (see Section 4.2). The initial states of compacted soils in the simulations are shown in Table 2. Since δ_p plays a pivotal role in controlling the volume changes, as elaborated in Section 2, Table 2 also provides the values of initial reference index, δ_{p0} to explore its effects on the compaction efficiency and the long-term performance of the compacted soils under traffic loads.

Table 2. Initial states of compacted soils in the numerical examples

Simulation	Initial degree of saturation, S_{r0}	Initial void ratio, e_0	Initial reference index, δ_{p0}
A1	0.2	0.65	0.9422
A2	0.3	0.65	0.9335
A3	0.4	0.65	0.9290
A4	0.5	0.65	0.9277
A5	0.6	0.65	0.9288
A6	0.7	0.65	0.9319
A7	0.2	0.70	0.6815
A8	0.3	0.70	0.6195
A9	0.4	0.70	0.5806
A10	0.5	0.70	0.5597
A11	0.6	0.70	0.5536
A12	0.7	0.70	0.5606
A13	0.2	0.75	0.4787
A14	0.3	0.75	0.4549
A15	0.4	0.75	0.4383
A16	0.5	0.75	0.4277
A17	0.6	0.75	0.4220
A18	0.7	0.75	0.4210

4.1 Compaction efficiency

The compaction efficiency is estimated by the normalised void ratio change $(e_0 - e_1)/(1 + e_0)$,

where e_1 is the void ratio at the end of compaction. If the value of $(e_0 - e_1)/(1 + e_0)$ is high, the compaction efficiency is considered to be high. Fig. 8 investigates the effects of e_0 on the compaction efficiency with various S_{r0}. Similarly, Fig. 9 explores how S_{r0} influences the compaction efficiency with various e_0. As shown in these figures, increasing either e_0 or S_{r0} while keeping the other variable same leads to higher compaction efficiency. Fig. 10 presents all 18 numerical simulations and investigates the impact of δ_{p0} on the compaction efficiency. It is shown that δ_{p0} has an inverse relationship with the compaction efficiency. In addition, it is arguable that δ_{p0} integrates the effects of e_0 or S_{r0}, and may serve as an integrated factor influencing the compaction efficiency.

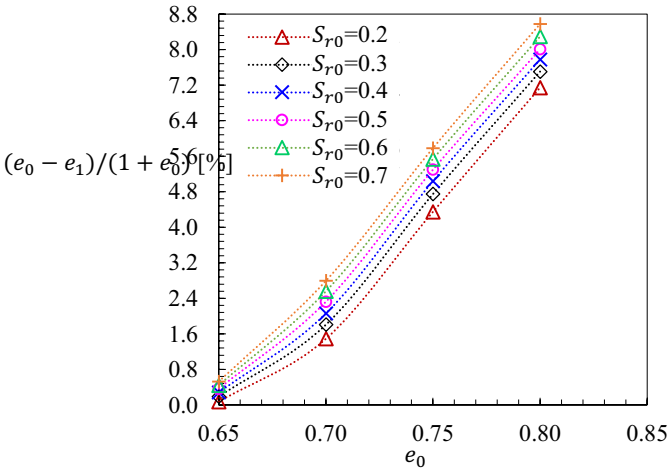

Fig. 8. Effect of initial void ratio on the compaction efficiency

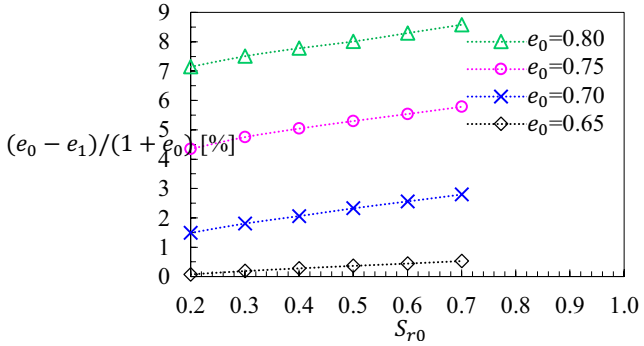

Fig. 9. Effect of initial degree of saturation on the compaction efficiency

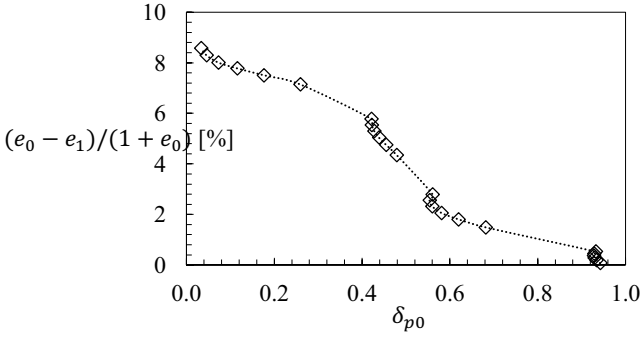

Fig. 10. Effect of initial reference index on the compaction efficiency

4.2 Long-term performance under repeated traffic loads

The long-term performance of compacted soils under repeated traffic loads is evaluated by the normalised void ratio change, $(e_1 - e_2)/(1 + e_1)$ (where e_2 is the void ratio at the end of the application of repeated traffic loads). To explore the effects of initial soil states and the compaction efficiency on the long-term performance of the compacted soils under repeated traffic loads, Fig. 11 presents the data of $(e_1 - e_2)/(1 + e_1)$ against $(e_0 - e_1)/(1 + e_0)$. When e_0 is high (e.g., $e_0 \geq 0.7$ in the presented examples), an initial reduction followed by an increase in $(e_1 - e_2)/(1 + e_1)$ can be observed when $(e_0 - e_1)/(1 + e_0)$ and S_{r0} increases. This observation indicates that the subsequent deformation under repeated traffic loads can be limited when compaction is efficiently conducted at a high initial void ratio and a low initial degree of saturation. However, if the initial degree of saturation is too high (e.g., $S_{r0} \geq 0.6$ in the examined cases), soil still deforms significantly under repeated traffic loads after compaction. When e_0 is low (e.g., $e_0 = 0.65$ in the presented examples), $(e_0 - e_1)/(1 + e_0)$ is low and increasing S_{r0} results in a greater value of $(e_0 - e_1)/(1 + e_0)$ and $(e_1 - e_2)/(1 + e_1)$. It implies that for a dense sample, 1) soil does not deform significantly during compaction as well as under repeated traffic; and 2) more deformations are generated during compaction and under repeated traffic if the initial degree of saturation increases.

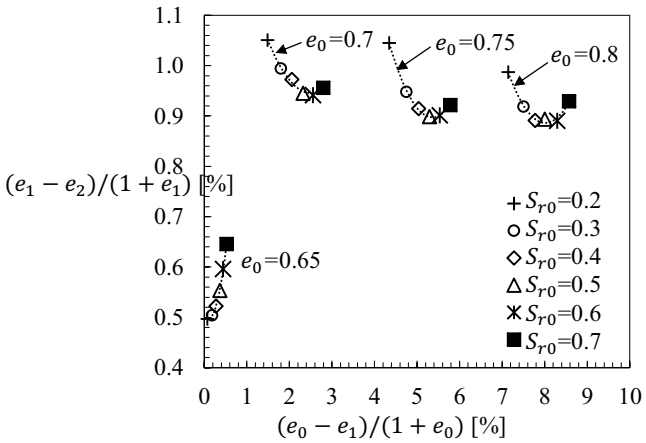

Fig. 11. Effect of compaction on the long-term performance of the compacted soils under repeated traffic loads.

5 Conclusions

We have presented a numerical approach for predicting the outcomes of IC, with several simplifying assumptions. The effectiveness of the approach has been demonstrated with the aid of several examples. By using the numerical approach, we have investigated the effects of the initial states of compacted soils on the compaction efficiency and the subsequent deformations of the compacted soils under repeated traffic loads. The analyses have demonstrated that the compaction efficiency can be increased by increasing either the

initial void ratio or the initial degree of saturation. In addition, the initial reference index, combining the effects of initial void ratio and initial degree of saturation on the compaction efficiency, can be considered an important factor for the practical design of relevant compaction parameters. Furthermore, it has been shown that efficient compaction can limit the subsequent deformations under repeated traffic loads if the soil is initially loose and the initial degree of saturation is not high.

Nonetheless, there is a scope for improving the accuracy of the numerical approach in predicting the outcomes of IC, such as treating the compaction and post-compaction processes as boundary value problems. This aspect will be addressed in future investigations by implementing the model in a finite element package.

The first author received the Monash University Graduate Scholarship (MGS) and the Monash International Tuition Scholarship (MITS) to conduct the research. The research is also part of a research project (Project No IH18.01.8) sponsored by the SPARC Hub at the Department of Civil Eng., Monash University funded by the Australian Research Council (ARC) Industrial Transformation Research Hub (ITRH) Scheme (Project ID: IH180100010). The financial and in-kind support received from Monash University and SPARC Hub are greatly acknowledged.

References

1. J.-L. Briaud and J. Seo, Texas A&M Univ. 1 (2003).

2. J. Kodikara, Can. Geotech. J. **49**, 1227 (2012).

3. J. Kodikara, C. Jayasundara, and A. N. Zhou, Comput. Geotech. **118**, 103332 (2020).

4. L. Chen, J. Ghorbani, C. Zhang, T. T. Dutta, and J. Kodikara, Comput. Geotech. **140**, 104446 (2021).

5. J. Ghorbani and D. W. Airey, Comput. Mech. **67**, 497 (2021).

6. J. M. Pestana, A Unified Constitutive Model for Clays and Sands, Massachusetts Institute of Technology, Cambridge, MA, 1994.

7. S. J. Wheeler, A. Näätänen, M. Karstunen, and M. Lojander, Can. Geotech. J. **40**, 403 (2003).

8. A. Raveendiraraj, Coupling of Mechanical Behaviour and Water Retention Behaviour in Unsaturated Soils, University of Glasgow, 2009.

9. J. M. Pestana and A. J. Whittle, Int. J. Numer. Anal. Methods Geomech. **23**, 1215 (1999).

10. A. Tarantino and E. De Col, Geotechnique **58**, 199 (2008).

11. J. M. Pestana and A. J. Whittle, Géotechnique **45**, 611 (1995).

12. D. W. Airey and J. Ghorbani, Comput. Geotech. **140**, 104402 (2021).

13. A. Tophel, J. P. Walker, T. T. Dutta, and J. Kodikara, Acta Geotech. (2022).

14. J. Ghorbani, M. Nazem, J. Kodikara, and P. Wriggers, Comput. Methods Appl. Mech. Eng. **384**, 113974 (2021).